13B.1 UPPER-TROPOSPHERIC STATIC STABILITY IN TROPICAL CYCLONES: OBSERVATIONS AND MODELING

Patrick Duran* and John Molinari
University at Albany, SUNY, Albany, NY

1. INTRODUCTION

Upper-tropospheric thermodynamic processes can play an important role in the structure and evolution of tropical cyclones (TCs.) In one theoretical model, for example, the maximum gradient wind speed at the top of the boundary layer is expressed as a function of the tropopause temperature (Emanuel and Rotunno 2011), and vortex amplification is partially controlled by the radial gradient of outflow temperature (Emanuel 2012).

Despite its potential importance, few observations of the upper-level potential temperature (θ) stratification of mature hurricanes exist. Recently, however, the Tropical Cyclone Intensity (TCI) Experiment (Doyle et al. 2017) deployed 244 high-altitude dropsondes within extraordinarily intense TC Patricia (2015). These observations, collected throughout Patricia's rapid intensification (RI) period, revealed dramatic static stability variations near the cold-point tropopause as the storm intensified (Duran and Molinari 2018).

This paper analyzes the physical mechanisms that might have produced the evolution observed in Hurricane Patricia, employing a budget analysis performed on a TC simulated in an idealized, axisymmetric framework.

2. MODEL SETUP AND METHODOLOGY

2.1 *Model Setup*

The numerical simulations were performed using version 19.4 of Cloud Model 1 (CM1; Bryan and Rotunno (2009), within a 3000-km-wide, 30-km-deep domain with a horizontal and vertical grid spacing of 1 km and 250 m, respectively. The equations of motion were integrated assuming an *f*-plane at 15°N latitude, with constant sea surface temperature of 30.5°C, consistent with that observed near Hurricane Patricia (Kimberlain et al. 2016). The vertical turbulence parameterization of Markowski and Bryan (2016) was employed, using an asymptotic mixing length of 100 m. The Thompson et al. (2004) microphysics scheme was used alongside the Rapid Radiative Transfer Model for GCMs (RRTMG) (Iacono et al. 2008), which computed the heating tendencies from longwave and shortwave radiation every two minutes. The model was initialized with a horizontally-homogeneous initial temperature and humidity field determined by averaging all Climate Forecast System Reanalysis (CFSR) grid points within 100 km of Patricia's center of circulation at 18 UTC 21 October 2015. An initial vortex was imposed, as described in Rotunno and Emanuel (1987; their Eq. 37), setting all parameters equal to the values used therein. The simulation produced a TC with maximum intensity similar to Hurricane Patricia's (Fig. 1), with a period of similarly rapid intensification. Model variables were output every minute for use in the budget analysis.

2.2 *Static Stability Budget Computation*

Assuming a dry atmosphere[1], the static stability can be expressed:

$$N^2 = \frac{g}{\theta}\frac{\partial \theta}{\partial z}, \quad (1)$$

where g is gravitational acceleration and θ is potential temperature. Taking the time derivative yields the static stability tendency:

$$\frac{\partial N^2}{\partial t} = \frac{g}{\theta}\frac{\partial}{\partial z}\frac{\partial \theta}{\partial t} - \frac{g}{\theta^2}\frac{\partial \theta}{\partial z}\frac{\partial \theta}{\partial t}, \quad (2)$$

where the potential temperature tendency, $\partial\theta/\partial t$, can be written as the sum of seven budget terms:

$$\frac{\partial \theta}{\partial t} = HADV + VADV + HTURB + VTURB + MP + RAD + DISS, \quad (3)$$

Each term on the right-hand size represents a θ budget variable, all of which are output by the model every minute. HADV and VADV are the

* *Corresponding author address:* Patrick Duran, Department of Atmospheric and Environmental Sciences, ES 338A, University at Albany, State University of New York, 1400 Washington Ave., Albany, NY 12222.
Email: pduran@albany.edu

[1] The validity of this assumption in the upper troposphere will be corroborated later in this section (see Fig. 2).

radial and vertical advective tendencies, HTURB and VTURB are the tendencies due to horizontal and vertical turbulence, MP is the tendency from the microphysics scheme, RAD is the radiative heating tendency, and DISS is dissipative heating. These terms are individually substituted into Eq. 2, yielding a contribution to the N^2 tendency from each of the terms every minute. These contributions are averaged over 24-hour periods and summed to yield an N^2 change over that time period. This "budget change" in N^2 is compared to the change directly output by the model for three 24-hour periods in Fig. 2. The N^2 tendency yielded by the budget computation is nearly identical to the actual change computed within the model over the same time period, indicating that the budget accurately captures the model variability.

Three of the budget terms dominate the N^2 tendency in the upper troposphere and lower stratosphere: advection, vertical turbulence and radiation (Fig. 3). Changes in the magnitude and location of the N^2 tendencies due to each of these processes determines the evolution of the tropopause-layer N^2.

3. RESULTS

3.1 *Static Stability Evolution*

Twenty-four-hour averages of N^2 and cold-point tropopause height are depicted in Fig. 4. The first 24 hours (Fig. 4a) were marked by a nearly flat tropopause with an N^2 maximum immediately above it. As the storm underwent RI (Fig. 1) during the 24-48-hour period (Fig. 4b), N^2 began to decrease within the developing eye, allowing the tropopause to rise in this region. Outside of the eye, meanwhile, the static stability increased just above the tropopause. These tendencies continued after the storm's maximum wind speed leveled off near 80 m s^{-1} (Fig. 1), with a further increase in tropopause height within the 30 km radius and increasing static stability outside of that radius just above the tropopause (Fig. 4c). This variability closely resembles that observed during Hurricane Patricia's RI (Duran and Molinari 2018). The analysis herein will focus only on the 24-48-hour period, during with RI took place.

3.2 *Static Stability Budget Analysis*

Within the 20-km radius, the RI period was marked by decreasing N^2 above 16 km and increasing N^2 below (Fig. 5a). These tendencies were forced almost entirely by advection (Fig. 5b).

Meanwhile outside of the 20-km radius, the layer above 17 km was dominated by stabilization and the layer below 17 km destabilization (Fig. 5a). The stabilization above 17 km was driven by a combination of vertical turbulence (Fig. 5c) and radiation (Fig. 5d), the sum of which outweighed the destabilizing influence of advection (Fig. 5b). Likewise, turbulence and radiation combined to produce the layer of decreasing static stability below 17 km, even though advection was strongly forcing stabilization throughout much of this layer.

3.5 *Conclusions*

An idealized, axisymmetric simulation of a rapidly-intensifying TC produced a static stability evolution similar to that observed in Hurricane Patricia (2015). A budget analysis executed in this framework indicates that turbulence and radiative heating tendencies both play important roles in determining the upper-tropospheric static stability evolution.

4. ACKNOWLEDGMENTS

We thank George Bryan for his continued development and support of CM1. We also acknowledge Jeffrey Kepert, Robert Fovell, and Erika Navarro for helpful conversations related to this work. This research was supported by NSF Grant #1636799.

5. REFERENCES

Bryan, G. H., and R. Rotunno, 2009: The maximum intensity of tropical cyclones in axisymmetric numerical model simulations. *Mon. Wea. Rev.*, **137**, 1770-1789.

Doyle, J. D., and Coauthors, 2017: A view of tropical cyclones from above: The Tropical Cyclone Intensity experiment. *Bull. Amer. Meteor. Soc.*, **98**, 2113-2134.

Duran, P., and J. Molinari, 2018: Dramatic inner-core tropopause variability during the rapid intensification of Hurricane Patricia (2015). *Mon. Wea. Rev.*, **146**, 119-134.

Emanuel, K., 2012: Self-stratification of tropical cyclone outflow. Part II: Implications for storm intensification. *J. Atmos. Sci.*, **69**, 988-996.

Emanuel, K., and R. Rotunno, 2011: Self-stratification of tropical cyclone outflow. Part

I: Implications for storm structure. *J. Atmos. Sci.*, **68**, 2236-2249.

Iacono, M. J,, J. S. Delamere, E. J. Mlawer, M. W. Shephard, S. A. Clough, and W. D. Collins, 2008: Radiative forcing by long-lived greenhouse gases: Calculations with the AER radiative transfer models. *J. Geophys. Res.*, **113**, D13103.

Kimberlain, T. B., E. S. Blake, and J. P. Cangialosi, 2016: Tropical cyclone report: Hurricane Patricia. National Hurricane Center. [Available online at www.nhc.noaa.gov].

Rotunno, R., and K. A. Emanuel, 1987: An air-sea interaction theory for tropical cyclones. Part II: Evolutionary study using a nonhydrostatic axisymmetric numerical model. *J. Atmos. Sci.*, **44**, 542-561.

6. FIGURES

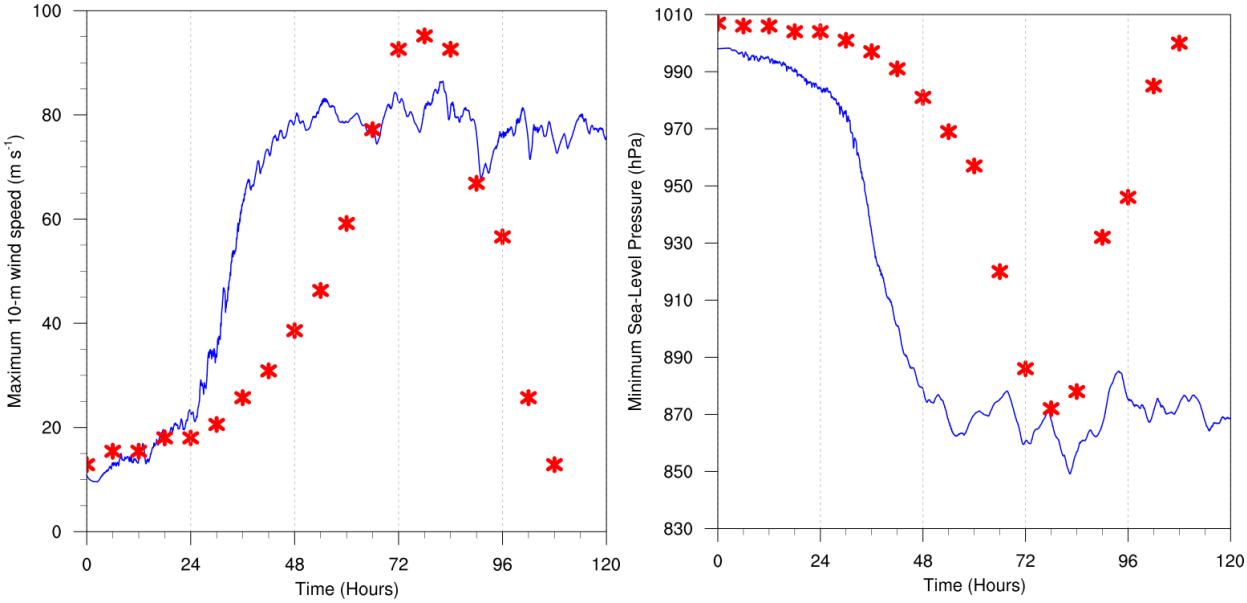

Figure 1. The maximum 10-m wind speed (left panel; m s^{-1}) and minimum sea-level pressure (right panel; hPa) in the simulated storm (blue lines) and from Hurricane Patricia's best track (red stars).

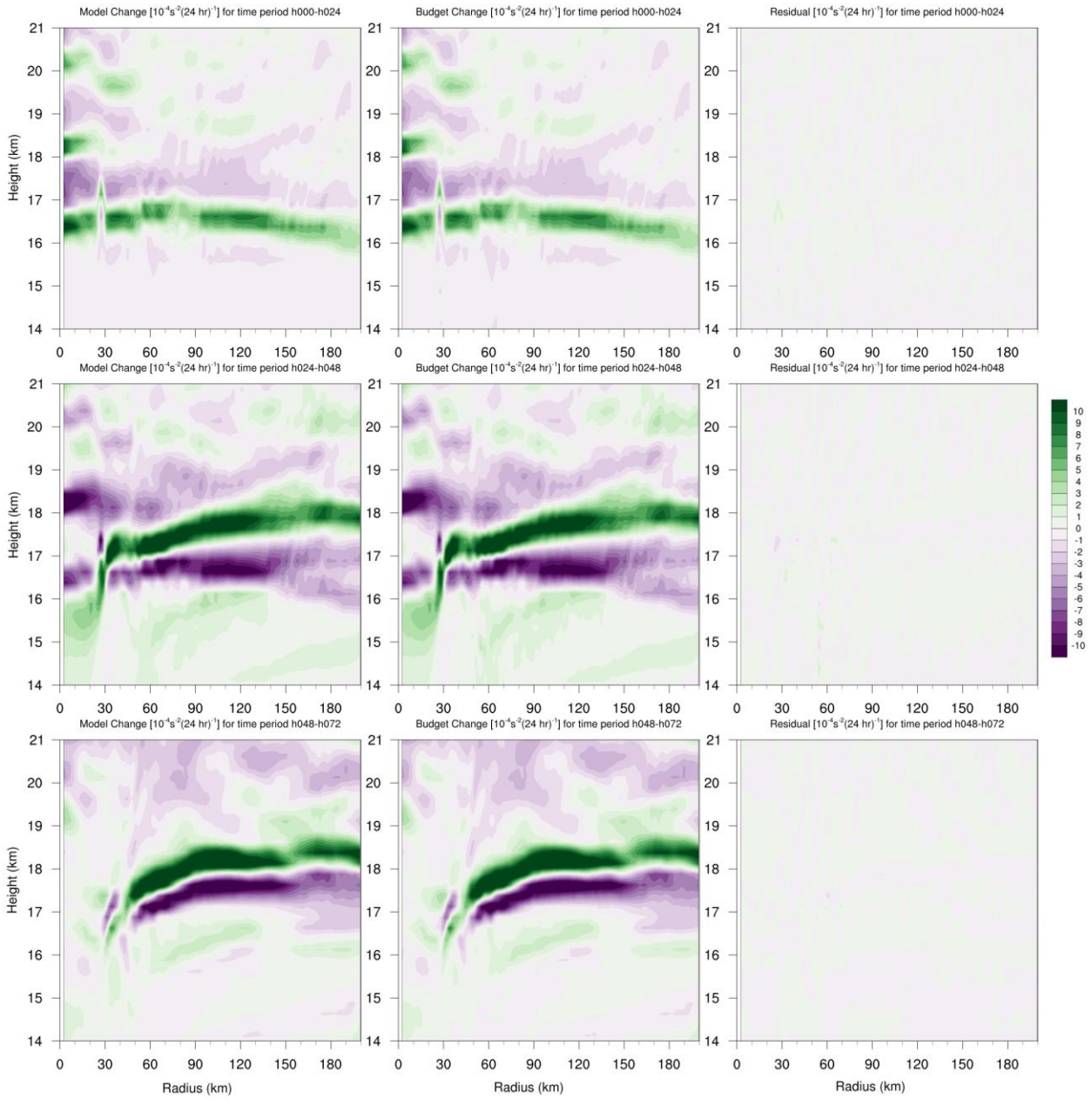

Figure 2. Left panels: Twenty-four-hour changes in squared Brunt-Väisälä frequency (N^2; 10^{-4} s^{-2}) directly output by the model over (top left) 0-24 hours, (middle left) 24-48 hours, (bottom left) 48-72 hours. Middle panels: N^2 changes over the same time periods computed using the static stability budget described in Section 2.2. Right panels: The residual over the same time periods, determined by subtracting the budget change (middle panels) from the model change (left panels).

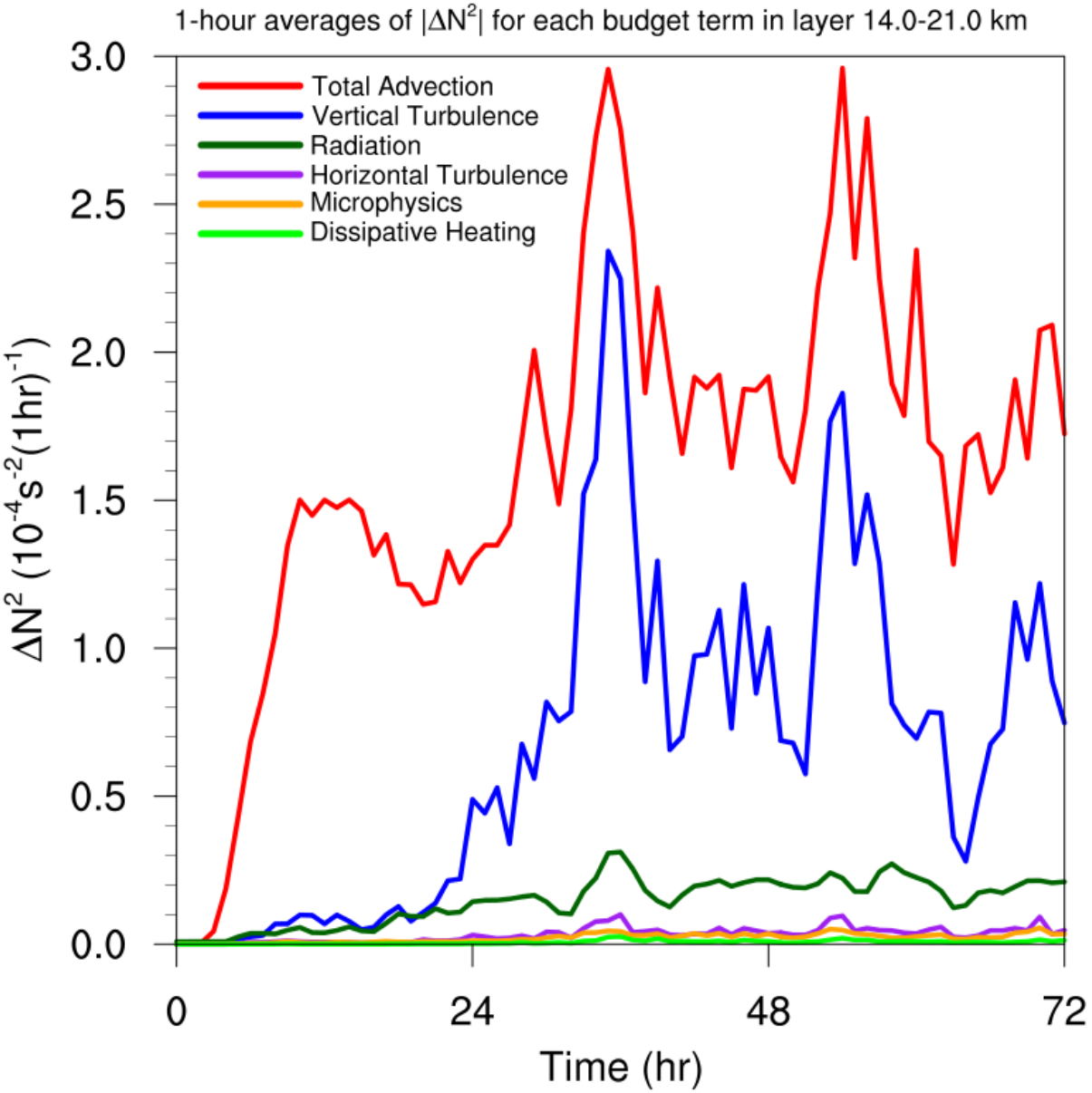

Figure 3. Time series of the contribution of each budget term to the squared Brunt-Väisälä frequency (N^2; 10^{-4} s^{-2}). For each term, the magnitude of the N^2 tendency is averaged temporally over 1-hour periods (using output every minute), and spatially in a region extending from 0 to 200 km radius and 14 to 21 km altitude.

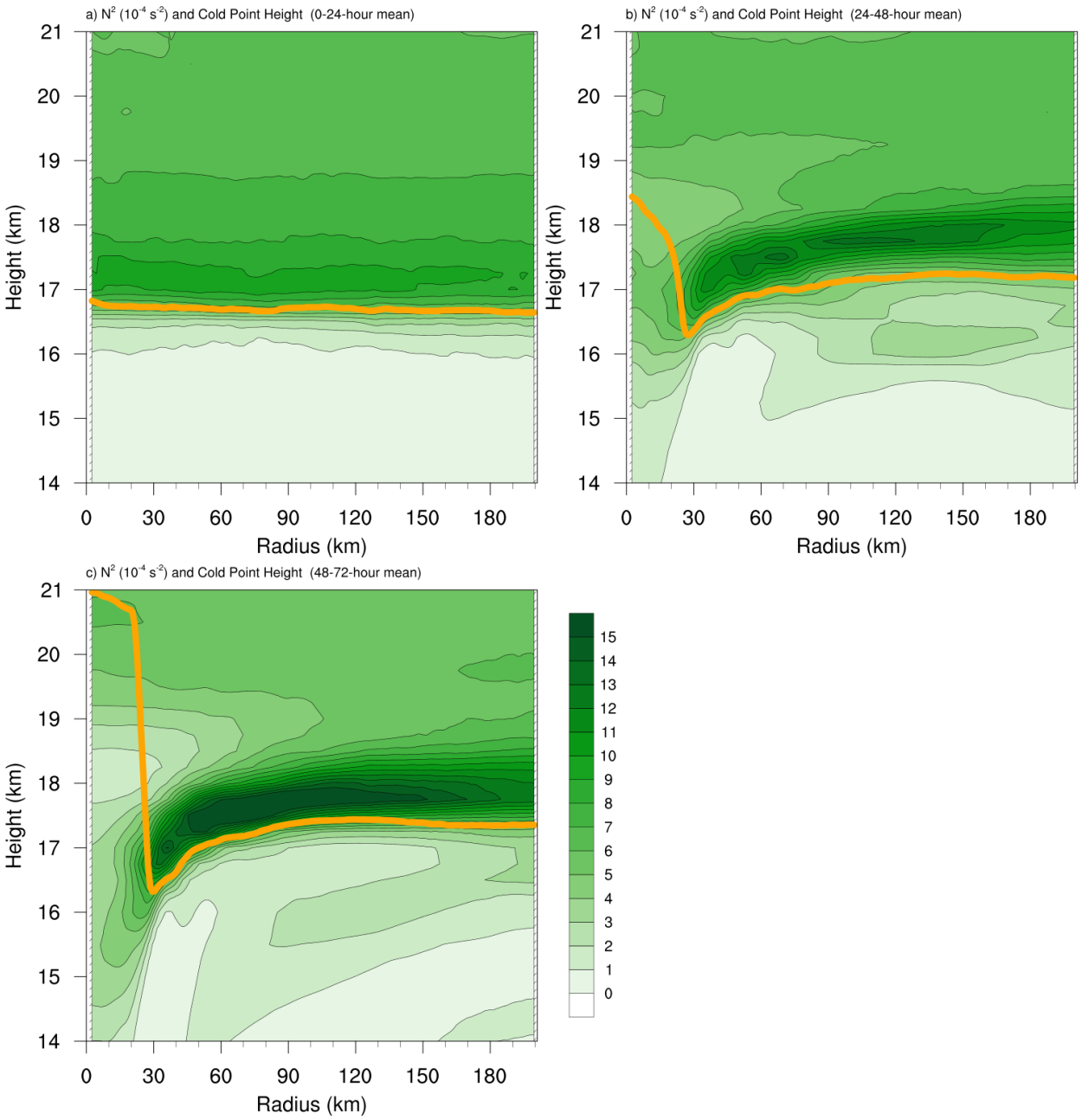

Figure 4. Twenty-four-hour averages of the squared Brunt-Väisälä frequency (N^2; 10^{-4} s^{-2}) over the (a) 0-24-hour period, (b) 24-48-hour period, and (c) 48-72-hour period. Orange lines represent the cold-point tropopause height determined by the mean temperature field over the same time periods.

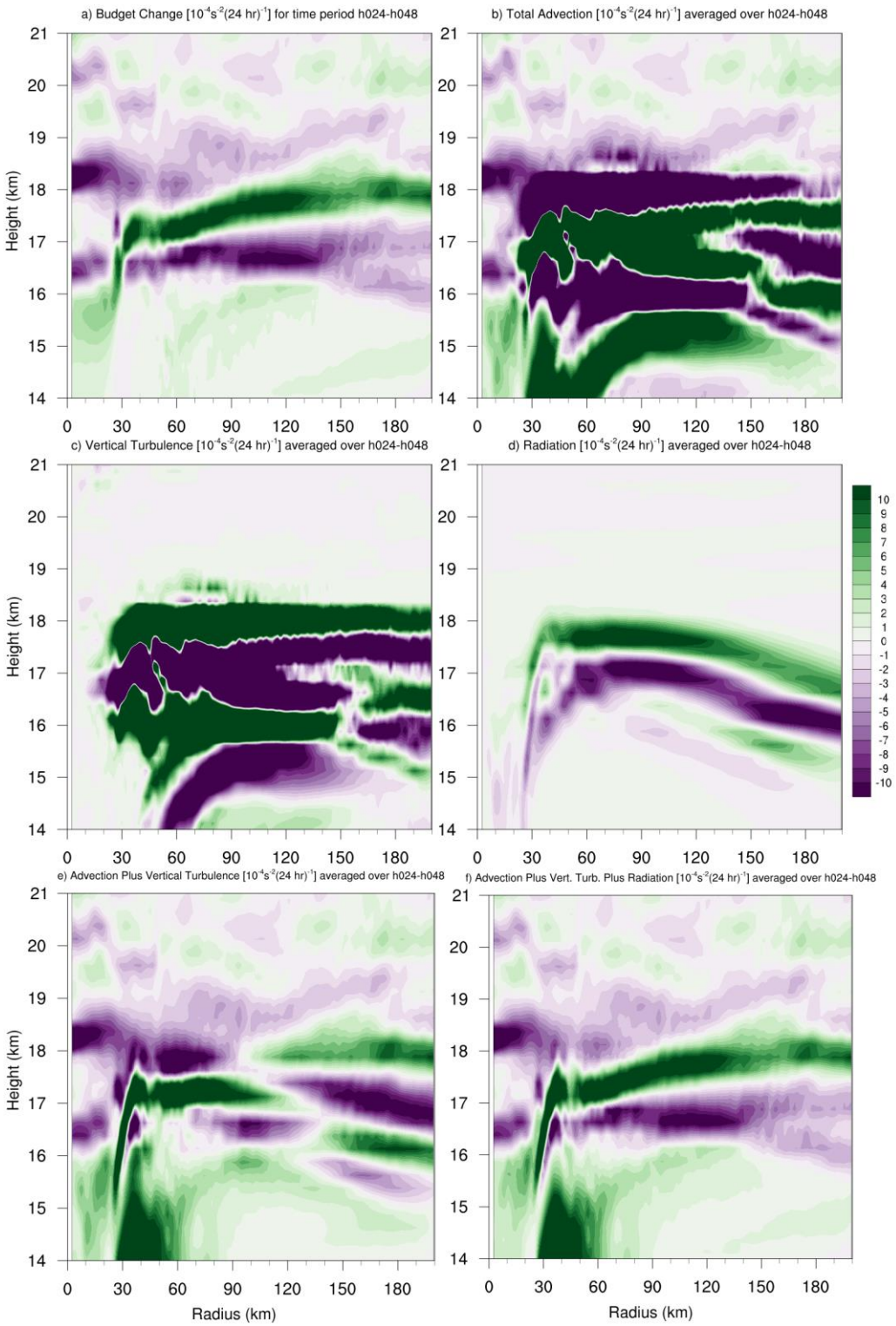

Figure 5. (a) Total change in squared Brunt-Väisälä frequency (N^2; 10^{-4} s^{-2}) over the 24-48-hour period, and the contributions to that change from (b) the sum of horizontal and vertical advection, (c) vertical turbulence, (d) longwave and shortwave radiation, (e) the sum of advection and vertical turbulence, and (f) the sum of advection, vertical turbulence, and radiation. Purple shading indicates regions of decreasing static stability during the period and greed shading indicates regions of increasing static stability.